

Simulation Study on Prediction of Urea Crystallization of a Diesel Engine Integrated after-Treatment Device

Menghua Wang, Xingyu Liu,* Jianjun Bao, Zhidan Li, and Jie Hu



Cite This: *ACS Omega* 2021, 6, 6747–6756



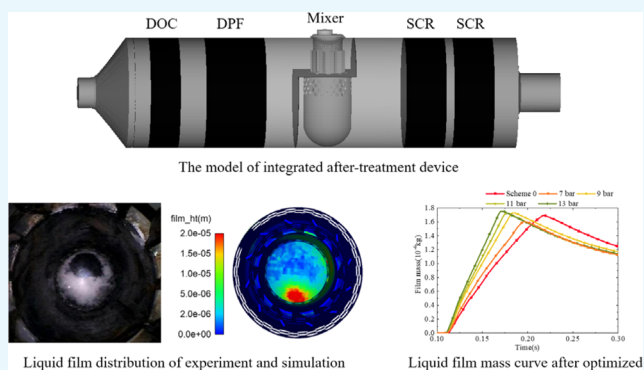
Read Online

ACCESS |

Metrics & More

Article Recommendations

ABSTRACT: An integrated after-treatment device model was established for our target engine based on the fluid simulation software (Converge), and simulation was performed to determine the NH_3 , temperature, and velocity uniformity at the front-end cross section of its SCR catalyst, urea deposition rate, liquid film mass of the mixer, and its positions under a low-load condition. Moreover, the structure of the mixer and injection pressure were optimized to improve the uniformity and reduce the liquid film mass. Our simulation results show the following facts: the liquid film is easily accumulated under a low-load condition and the structure of the mixer and the injection pressure significantly affect the urea deposition rate and uniformities and accumulation masses of the liquid film. As a result, our final optimization results indicate that the mass of the NH_3 and the NH_3 uniformity at the front-end cross section of the SCR catalyst increase by 2.83 times and 5.65%. The urea deposition rate and the cumulative mass of the liquid film fall by 4.82 and 10.4%, respectively. This study has certain theoretical guiding significance for the optimal design of this type of after-treatment devices.



1. INTRODUCTION

Diesel engines have advantages such as high thermal efficiency, wide power coverage, and good durability, but solution of their emission issues shall be an urgent and important demand for construction of national ecological civilization. At present, the technical route including the in-engine evolution technology and integrated after-treatment device is integrated with various single-item systems such as DOC, DPF, and SCR^{1–3} taken to meet the national VI diesel engine emission regulations.⁴ However, there are still some issues in its application processes, for example, NO_x emission exceeds its standard requirements⁵ and ammonia is leaking, because NH_3 and exhaust gas are mixed unevenly due to its compact structure. Especially, the most serious issue is urea crystallization which will result in the following issues such as insufficient vehicle power and excessive emission.⁶ Thus, analysis and optimization shall be necessary for these key issues.

Model simulation was carried out to analyze effects of nozzle parameters on the concentration distribution of the inlet section of the catalyst carrier.⁷ A static urea spray crystallization test platform was established, and the relationship between the minimum amount of urea spray wall collision and the risk of urea crystallization was presented.⁸ The urea crystallization was studied in an SCR system under low flow rate and temperature.⁹ Analysis of causes for the urea crystallization of the vanadium-based catalyst was performed.¹⁰ The interaction between urea spray droplets and the wall

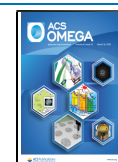
surface was studied.¹¹ In the study of urea crystallization byproducts, research mentioned in ref 12 was carried out to study the formation and byproducts by thermogravimetric analysis and differential scanning calorimetry and research mentioned in refs^{13,14} was carried out to study the distribution of byproducts by numerical simulation, and the mixer structure was optimized.

In summary, various aspects of Urea-SCR systems were currently explored in many studies which can act as the foundation for research and prediction of the SCR urea crystallization mechanism and crystallization risk of diesel engines. However, research on urea spray characteristics and crystallization is rarely carried out for any integrated after-treatment so far. Thus, a certain integrated after-treatment device was modeled here to study the urea spray atomization and mixing processes by means of the numerical simulation method and performing predictive analysis of the urea decomposition rate, uniformities, cumulative masses, and formation locations of the liquid film under high and low

Received: November 30, 2020

Accepted: December 30, 2020

Published: March 3, 2021



loads. Finally, an optimized design is performed based on the analysis results to reduce the risk of urea crystallization in an integrated after-treatment device but provides a certain theoretical basis for improvement of the SCR reaction efficiency.

2. EXPERIMENTAL SECTION

2.1. Experimental System. This experimental system is composed of the thermodynamic system and an integrated after-treatment system. The thermodynamic system consists of an intake pump, air flowmeter, and natural gas supply system. The integrated after-treatment system consists of a urea pump, urea injection control system, urea nozzle, and integrated after-treatment device. The urea crystallization experimental system is shown in Figure 1. The thermodynamic system simulates the temperature and flow rate of engine exhaust by controlling the combustion volume of natural gas and pumping in quantitative air.

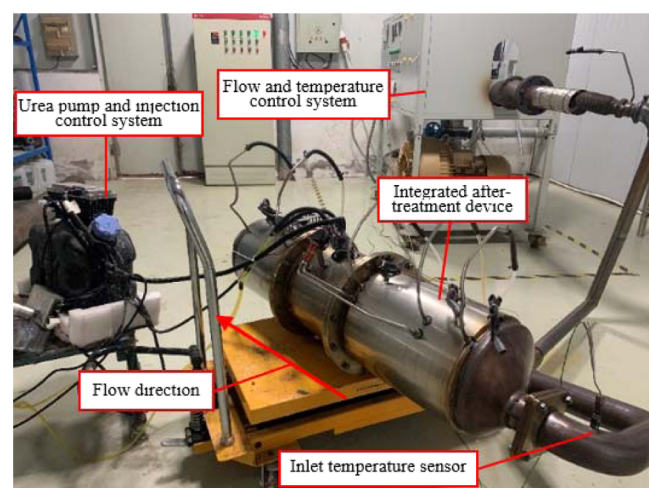
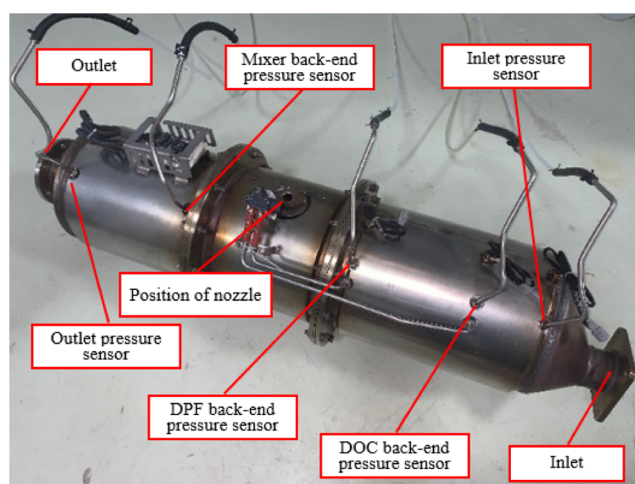


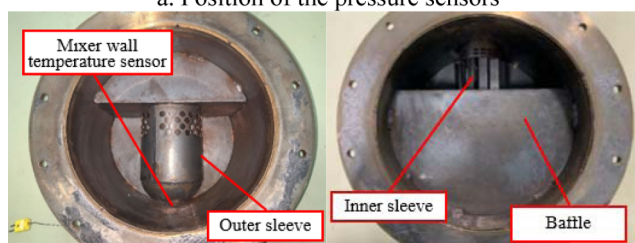
Figure 1. Experimental system.

Figure 2 shows the integrated after-treatment device and the position of the sensors. The total length of the device is 1219 mm, the inner diameter is 287 mm, the front end is the exhaust inlet (radius: 38.5 mm), and the back end is the exhaust outlet (radius: 49.5 mm). Figure 2a shows the position of the pressure sensors and the position of the urea nozzle. The urea nozzle (three-hole injection) is primarily used to atomize and spray urea. Its spray hole diameter is 186 μm . Three holes are distributed in a circle (diameter: 1.9 mm; spacing angle: 120°). Five pressure sensors measure the inlet (DOC front end) pressure, DOC back-end (DPF front end) pressure, DPF back-end (mixer front end) pressure, mixer back-end (SCR front end) pressure, and outlet (SCR back-end) pressure. The pressure drop between the catalyst and mixer can be obtained by subtracting the measured pressure values.

The mixer is shown in Figure 2b, which can fully spray urea and mix urea and exhaust gas to ensure the smooth progress of the subsequent reactions. The mixer is directly equipped below the urea nozzle from whose top the urea solution is sprayed into the inner sleeve of the mixer which is primarily made up of inner and outer sleeves and a baffle dividing the mixer tube into the upper and lower parts; thus, gas can only pass through the inner sleeve and the spray urea can be mixed here; the mixture finally enters the SCR catalyst part through the lower



a. Position of the pressure sensors



b. Mixer and position of wall temperature sensor

Figure 2. Integrated after-treatment device and the position of the sensors. (a) Position of the pressure sensors. (b) Mixer and position of the wall temperature sensor.

outer sleeve to exit the system after reactions. The temperature sensor is fixed at the bottom of the outer sleeve to measure the wall temperature of the mixer during urea injection. The inlet temperature sensor is indicated in Figure 1.

2.2. Experiment Condition and Methods. The previous research¹⁵ indicates that urea crystals are closely related to the exhaust gas flow rate and temperature and the urea injection amount; research^{16–18} verified the CFD model by the pressure drop of catalysts, NO_x conversion efficiency, wall temperature, and urea crystallization position, and study¹⁹ indicates that the surface reactions on the relevant catalyst result in only a small result difference for study of the flow field distribution in an after-treatment system. Thus, the effect of the catalyst on the back pressure rather than the relevant surface reactions was taken into account here. Therefore, this experiment is designed to measure the back pressure of catalysts under steady flow, the wall temperature of the mixer, and the position of urea crystallization; the effectiveness of the CFD model is verified by the abovementioned experimental results.

In order to observe the obvious phenomenon of urea crystallization, the engine condition shown in Table 1 is

Table 1. Experiment Condition

	OP1
engine speed (rpm)	1700
load (%)	10
exhaust mass flow rate (kg/h)	393.12
exhaust flow temp (K)	461.02
urea spray mass rate (g/s)	1.35
urea spray pressure (bar)	5

selected and the urea–water–solution (UWS) is injected. The working condition is the low-load condition of the diesel engine with low exhaust temperature and low exhaust flow rate. This experiment is divided into two parts, experiment 1: the exhaust temperature and flow rate are set according to the boundary conditions shown in Table 1 and the pressure value is recorded after the temperature and flow rate become stable and experiment 2: after the temperature and flow rate are stable, we start to record temperature values and start to spray urea. The duration of urea injection lasts for 1 h. After urea injection, the system is closed and the integrated after-treatment device is left in the atmospheric environment; then, urea crystallization is checked and the relevant experimental data are recorded.

3. MODEL AND MATHEMATICAL MODEL

3.1. Geometric Model of an Integrated after-Treatment Device. Our integrated after-treatment device is schematically shown in Figure 3. The whole device is

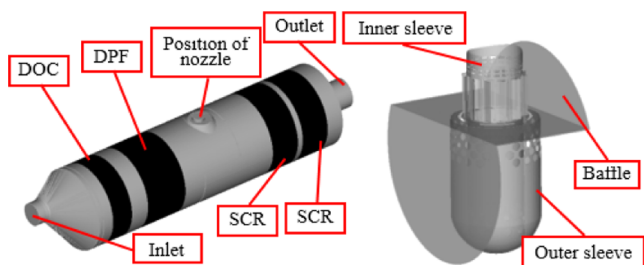
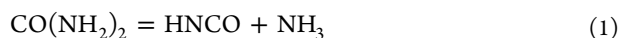


Figure 3. Model of the integrated after-treatment device.

simplified as a hollow cylinder with the same inner diameter, and the geometric size is consistent with the real device. The dark part represents the catalyst part including DOC, DPF, and two SCR blocks from the front to the back. The geometric model of the mixer is shown in the right figure, which is installed below the urea nozzle.

3.2. Molten Solid Urea Decomposition. The molten solid approach is chosen to model the decomposition of a UWS; the Frossling correlation models the evaporation of the water in the UWS, while an Arrhenius correlation models the decomposition of the urea in the UWS.^{20,21} In the molten solid approach, urea decomposes to gaseous ammonia and isocyanic acid. Equation 1 shown below gives the formula for the decomposition



The Arrhenius correlation (given in Equation 2) models this decomposition by computing the time rate of change in droplet radius as a function of a prefactor, the activation energy, the droplet temperature, and the density of urea. The correlation is

$$\frac{dm_d}{dt} = 2\pi r_d A \exp\left(-\frac{E_a}{RT_d}\right) \quad (2)$$

where r_d is the droplet radius, A is the prefactor, E_a is the activation energy, T_d is the droplet temperature, and m_d is the droplet mass. For this model, the droplet density is equivalent to the urea density.

3.3. Flow and Porous Media Model. In the whole area, the exhaust gas flow follows the mass, momentum, and energy

conservations and conforms to the characteristics of turbulent flow.²² Thus, the k – ϵ model was selected for turbulence simulation.²³

Because the space utilization rate is high and the distribution of each catalyst is compact in an integrated after-treatment device, catalysts can greatly affect the back pressure. The DOC, DPF, and SCR catalysts were set as porous media regions to simulate the effects of actual catalysts on the exhaust back pressure. The permeability equation is expressed as

$$K_1 = \alpha_i |\nu_i| + \beta_i \quad (3)$$

where K_1 represents the permeability of the material, α_i and β_i represent the coefficients which determine the material permeability in the direction of gas flow, and ν_i represents the velocity of the gas flow, whose unit is in m/s.

3.4. Urea Spray and Liquid Film Formation Model. While the urea spray model was established, the Rosin-Rammler model distribution was selected to simulate the droplet size change. Its distribution coefficient was set as 3.5. The turbulent diffusion of the droplet was performed by means of the O'Rourke model. The Taylor Analogy Breakup model was selected, and it is assumed that droplets only collide twice.²⁴ The atomized droplets undergo the complex processes of pyrolysis and hydrolysis to generate ammonia gas while they are sprayed into the urea nozzle. It is assumed that urea and aqueous solution are uniformly mixed in each droplet. The multicomponent Frossling droplet evaporation model, urea decomposition mechanism, Kuhnke liquid film/splash model, and liquid film evaporation model were selected to simulate this complex process.

Research²⁵ was carried out using an analytical model for the heat transferred which was developed by Wruck and Renz²⁶ who calibrate with their own experiments of isopropanol drops impinging on a NiCr surface, given as

$$Q_{w-d} = C_{Wruck} \cdot A_{cont} \frac{2\sqrt{t_{dc}}}{\sqrt{\pi}} \frac{b_w b_d}{b_w + b_d} (T_w - T_d) \quad (4)$$

where A_{cont} is the contact wall, t_{dc} is the direct contact time, T_w is the wall temperature, T_d is the droplet temperature, and b_w and b_d are the thermal effusivities of the droplet and the wall, respectively.

Research²⁵ indicates that Wruck and Renz experiments²⁶ use isopropanol for calibration, whereas the liquid of current interest is UWS. The different liquid properties may explain why a new factor (C_{Wruck}) was needed, and the C_{Wruck} was set to 1.7 for this CFD model to match experimental data.

3.5. Boundary Conditions and Spray Initialization. The exhaust temperature and flow rate set in the simulation process are consistent with the experimental condition OP1. The urea solution (mass fraction: 32.5%) is sprayed at 5 bar and 5 Hz. The total simulation duration is 0.3 s. Urea is injected at a time of 0.1 s. The urea injection duration is determined by the total urea injection mass and urea injection pressure, which is 0.1 s. The first period of 0.1 s is used to observe whether the gas flow can reach a stable state. Figure 4 shows the spray characteristics.

3.6. Distribution Uniformity Coefficient and Urea Deposition Rate. The SCR reaction mechanism indicates that the hydrolysis and pyrolysis of urea droplets that finally participate in the denitration reaction generate NH_3 whose concentration and distribution uniformity is the most important influencing factor in the entire SCR system. The

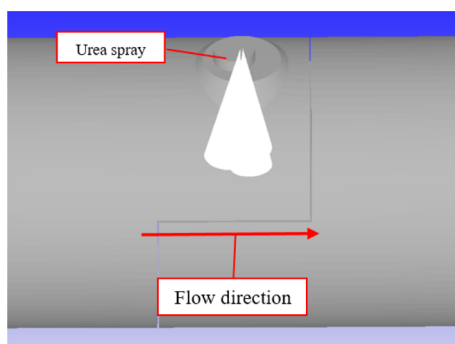


Figure 4. Spray characteristics.

uneven distribution of NH_3 will cause the changing degrees of reaction in different channels. NH_3 may be excess or insufficient in some channels so that the denitration efficiency may fall and NH_3 can be leaking. Also, the temperature uniformity at the front end of the SCR catalyst that is equally important as the NH_3 uniformity can result in different degrees of heating of the catalyst which may be aging in different positions and different degrees after a period of operation time so that its service life can be shortened. If the flow uniformity is poor, the gas flowing into the catalyst pores may be unevenly distributed. Also, the catalyst efficiency and service life will be affected. The uniformity coefficient of the front-end section of the catalyst is often used as an evaluation factor,²⁷ which is defined as

$$\gamma = 1 - \frac{1}{2n} \sum_{i=1}^n \frac{\sqrt{(\alpha_i - \alpha)^2}}{\alpha} \quad (5)$$

where α_i represents the NH_3 concentration, temperature, and velocity at a certain point of the front-end section of the catalyst and α represents the average NH_3 concentration, temperature, and velocity of the cross section. The flow will be more evenly distributed, and its uniformity will be better while γ goes close to 1.

At the end of the simulation, the percentage of the total mass of the liquid film to the total mass of urea injection is defined as the urea deposition rate, which is used to evaluate the performance of the mixer. The correlation is

$$\beta_{\text{Urea}} = \frac{m_{\text{film}}}{m_{\text{Urea}}} \times 100\% \quad (6)$$

where β_{Urea} is the urea deposition rate, m_{film} is the mass of the liquid film, and m_{Urea} is the total mass of urea injection.

4. RESULTS AND DISCUSSION

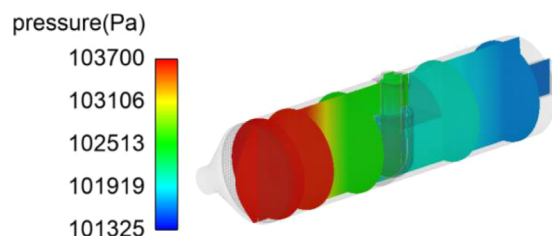
4.1. Experimental and Simulation Results of OP1.

4.1.1. Back Pressure Analysis. The back pressure measurements of each catalyst and the fitted permeability coefficients for DOC, DPF, and SCR catalysts are shown in Table 2.

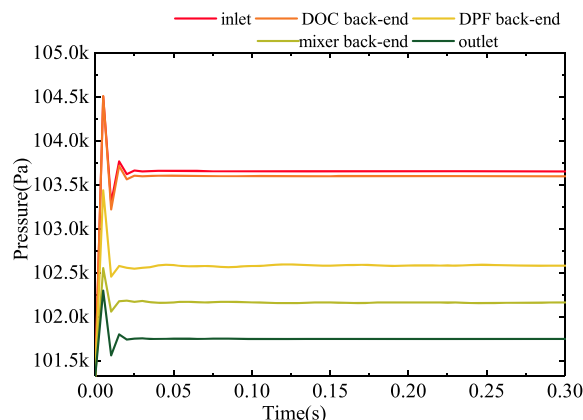
Table 2. Catalyst Permeability Coefficient

	α (kg/m ⁴)	β (kg/m ³ ·s)
DOC	18.92	458.87
DPF	1282.6	2495.71
front SCR	424.76	716.27
back SCR	424.76	716.27

Figure 5a shows the pressure cloud diagrams of each catalyst and the longitudinal section of the device in the simulation



a. pressure cloud diagrams of each catalyst and the longitudinal section of the device



b. Simulation pressure value of each section

Figure 5. Results of simulated pressure values. (a) Pressure cloud diagrams of each catalyst and the longitudinal section of the device. (b) Simulation pressure value of each section.

process. The position of the cross section is consistent with the position of the pressure sensors in the experiment. Figure 5b shows the curves of the average pressure value on each section with the simulation time; the pressure values of each cross section reach stability at the simulation time 0.025 s. The simulation pressure values are 103653.38, 103598.43, 102583.73, 102158.28, and 101746.93 Pa; the experimental pressure values are 103642.55, 103586.44, 102583.87, 102165.35, and 101748.33 Pa, respectively. The pressure drop of catalysts and the mixer between simulation and experiment is shown in Table 3, indicating that the pressure drop between the catalyst and mixer is well fitted and the error is less than 2%.

Table 3. Pressure Drop between Simulation and Experiment

	experiment (Pa)	simulation (Pa)	error (%)
DOC	56.11	55.18	1.66
DOF	1002.57	1014.48	-1.19
Mixer	418.52	425.45	-1.65
SCR	417.01	411.35	1.36
total	1894.22	1906.45	-0.65

4.1.2. Results of Wall Temperature. The experimental and simulated wall temperature curves with time are shown in Figure 6; the simulation value is well fitted with the experimental value, which is stable at 462 K before urea injection and decreases when urea is sprayed. The final simulation and experimental values are stable at 338 K.

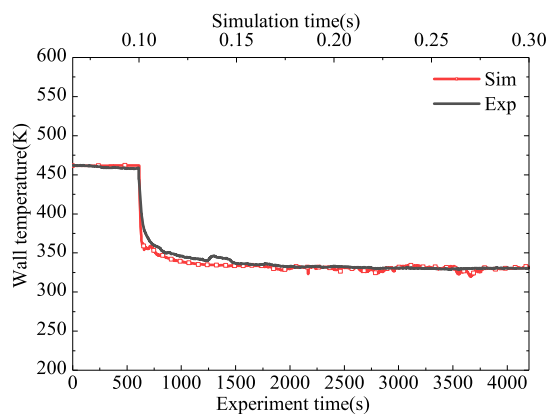


Figure 6. Results of wall temperature.

4.1.3. Results of the Film Mass and Urea Deposition Rate.

Figure 7 shows the liquid film distributions of the outer and

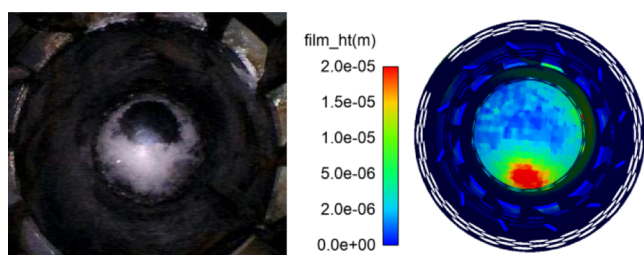


Figure 7. Liquid film distribution.

inner sleeves of the mixer under OP1, where the gas flows leftward. The experimental result shows that most of the urea deposited at the bottom of the spherical shell of the outer sleeve, only a thin layer of the urea crystal is found on the wall of the inner sleeve, and a small amount of crystal is generated on the baffle. The simulated liquid film thickness is basically consistent with the experimental results, indicating that the model has certain prediction accuracy.

Figure 8 (the cumulative mass of the liquid film vs the simulation time) indicates that the liquid film mass increases sharply to accumulate the liquid film, while urea is sprayed under a low-load condition. While the urea spraying stops, a small part of the liquid film will continue to dissipate under the action of gas flow and wall temperature and 1.25×10^{-4} kg of

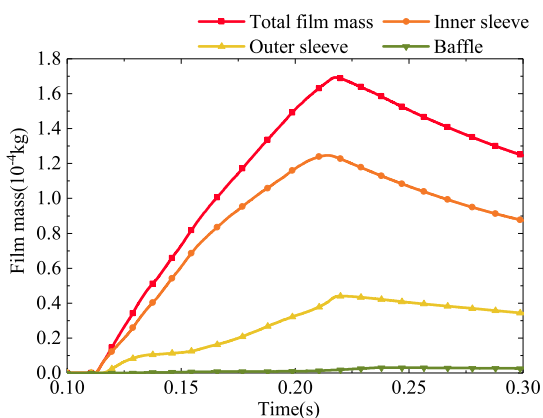


Figure 8. Film mass of each part of the mixer.

the liquid film will remain at the end of the cycle. The urea deposition rate is 46.3%.

At the end of the simulation, the film mass of the inner sleeve is more than that of the outer sleeve. In the experiment, urea crystallization will move downward under the influence of gravity, but this influence is not obvious in the simulation process.

4.1.4. Results of the Uniformity, the NH_3 Mass, and the NH_3 Volume Fraction at the Front-End Cross Section of the SCR Catalyst. The mass of NH_3 and the NH_3 volume fraction at the front end of the SCR catalyst are shown in Figure 9. In

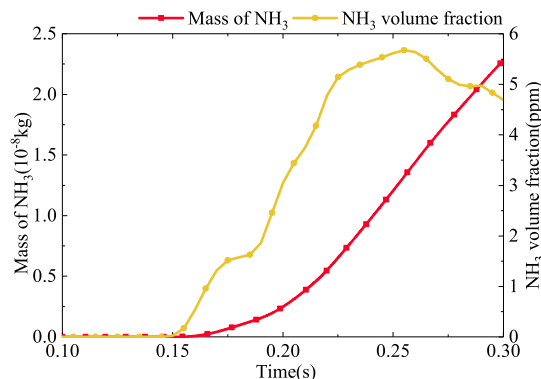


Figure 9. Mass of NH_3 and the NH_3 volume fraction at the front-end cross section of the SCR catalyst.

the case of a simulation time of 0.255 s, the NH_3 volume fraction of the SCR front-end cross section can reach a peak value. Instead, the low temperature and low flow ensure that NH_3 remains in the system and only 2.28×10^{-8} kg NH_3 passes through the front-end section of SCR at the end of the cycle.

For convenience of observation, the moment when the volume fraction of NH_3 at the front end of the SCR peaks under OP1 is selected (at the simulation time 0.255 s). The SCR front-end section cloud is shown in Figure 10, and the corresponding uniformity coefficient curves are shown in Figure 11. The uniformity coefficient of NH_3 is stable after 0.25 s, which is about 0.8971, indicating that there is still a large space for optimization, while the uniformity coefficients of velocity and temperature are all above 0.95.

4.2. Simulation Results of Mixer Structure Optimization. The previous results indicate that accumulation of the liquid film is more serious on the mixer under a low-load condition (low flow rate and temperature). For reducing the crystallization risk but also improving the anticrystallization ability of the integrated after-treatment system, the mixer structure and the injection pressure are optimized.

The optimization scheme of the mixer structure is as follows: (1) the diameter of the eight rows of small holes in the inner sleeve is changed to 10 mm and there are 18 evenly distributed holes in each circle and (2) the diameter of four rows of small holes in the outer sleeve is changed to 10 mm, whose arrangement is as follows:

- scheme 0: the scheme that was not optimized before;
- scheme 1: small holes are evenly distributed in the outer wall (namely, they are fully occupying the circumference);
- scheme 2: small holes are distributed in a total of 75% of the circumference;

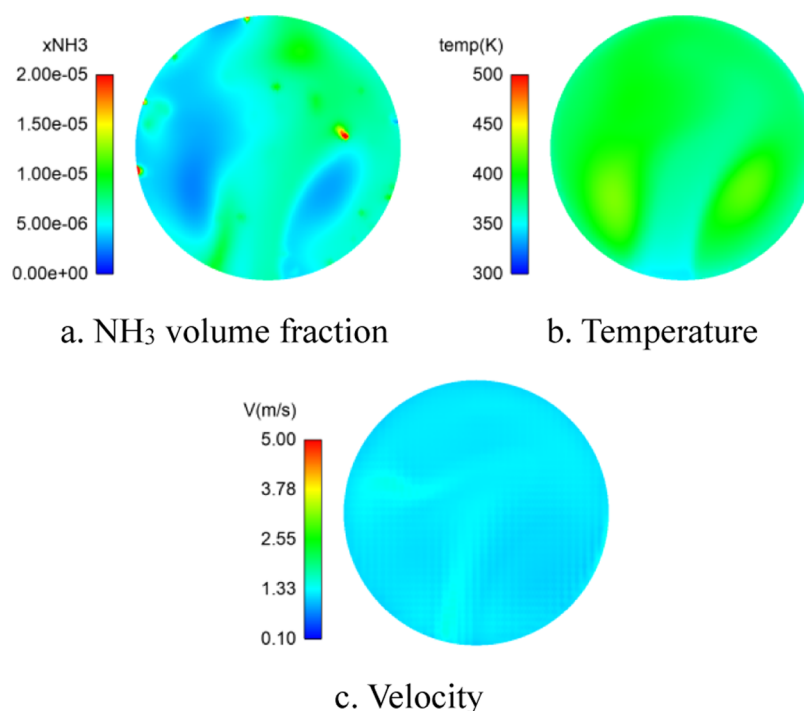


Figure 10. NH_3 volume fraction, temperature, and velocity cloud diagrams. (a) NH_3 volume fraction. (b) Temperature. (c) Velocity.

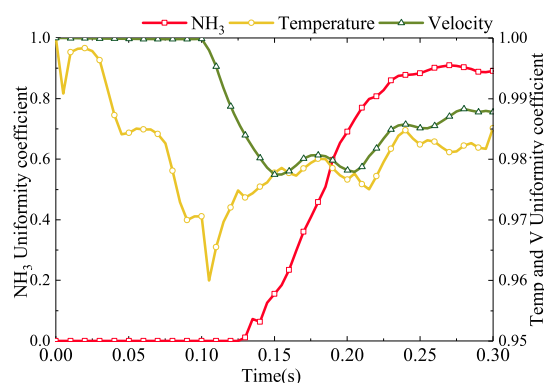


Figure 11. Uniformity coefficient curve.

scheme 3: small holes are distributed in a total of 50% of the circumference; and

scheme 4: small holes are distributed in a total of 25% of the circumference.

The abovementioned schemes are schematically shown in Figure 12, where Figures a, b, c, d, and e correspond to arrangements where the small holes below are distributed in the inner sleeve and layouts of small holes in schemes 1, 2, 3, and 4.

4.2.1. Results on the NH_3 Mass and the NH_3 Volume Fraction at the Front-End Cross Section of the SCR Catalyst. Figure 13 shows the relations (the total NH_3 mass at the front-end cross section of the SCR catalyst vs time) of each scheme, which indicates that all schemes have higher NH_3 mass and the NH_3 volume fraction at the front-end cross section of the SCR catalyst compared to the scheme without optimization. At the end of the simulation, the total NH_3 mass of schemes 1, 2, 3, and 4 are 6.58 , 5.14 , 4.23 , and 2.92×10^{-8} kg, respectively. With the ratio of small holes distributed decreasing, the NH_3 mass and the volume fraction will also decrease. Scheme 1 is the highest among all schemes.

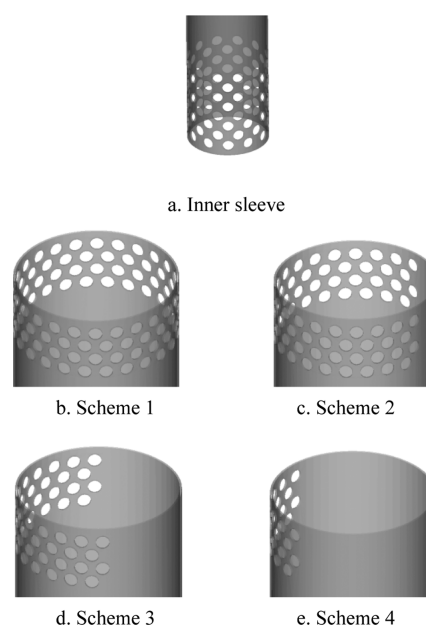


Figure 12. Mixer optimization scheme. (a) Inner sleeve. (b) Scheme 1. (c) Scheme 2. (d) Scheme 3. (e) Scheme 4.

4.2.2. Results on the Uniformity. Figure 14 shows the uniformity coefficient of each scheme. Compared with the original unmodified structure, the velocity uniformity of each scheme falls to varying degrees except scheme 1. The fact that temperature uniformity is maintained above 0.97 indicates that changing the structure to this type of after-treatment system dose basically does not affect its temperature uniformity. Before 0.23 s, the NH_3 uniformity coefficient of scheme 3 is higher than that of scheme 1; after 0.23 s, the NH_3 uniformity coefficient of scheme 1 and scheme 3 is basically the same, which is the highest among all schemes.

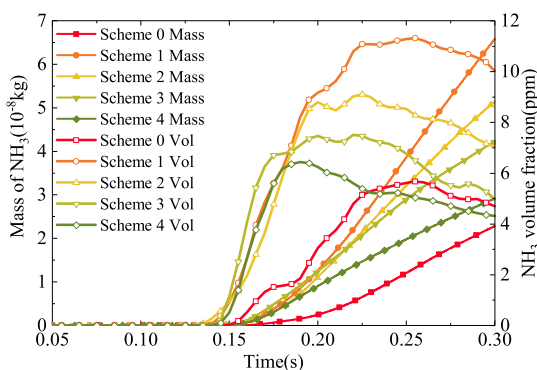
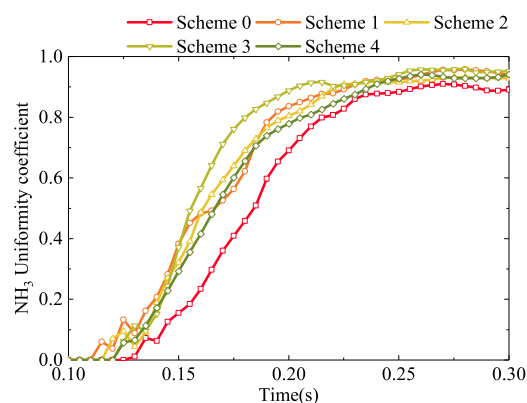
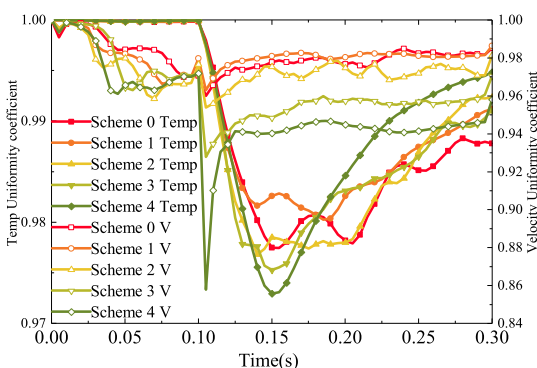


Figure 13. Mass of NH_3 and the NH_3 volume fraction at the front-end cross section of the SCR catalyst for each scheme.



a. NH_3 uniformity coefficient



b. Temperature and velocity uniformity coefficient

Figure 14. Uniformity coefficient curve for each schemes. (a) NH_3 uniformity coefficient. (b) Temperature and velocity uniformity coefficient.

4.2.3. Results on the Film Mass. The relations (film mass vs time for each scheme, Figure 15.) indicates that schemes 1, 2, and 3 can reduce the liquid film mass, whose cumulative mass are 1.21 , 1.17 , and 1.19×10^{-4} kg, respectively. Scheme 4 has a slight growth of cumulative liquid film mass compared to the scheme without changing its mixer structure because gas flows out of the left small holes so as to weaken the gas fluidity to a certain extent; thus, the cumulative mass of the liquid film grows.

To sum up, scheme 1 has the highest NH_3 mass, NH_3 volume fraction, and NH_3 uniformity coefficient, except the film mass being higher than that of schemes 2 and 3. Scheme 1 is optimal among the four schemes. Thus, the injection

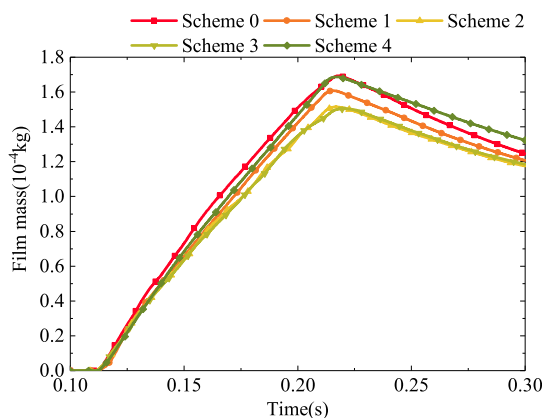


Figure 15. Mass of the film in each scheme.

pressure is optimized based on the mixer structure of scheme 1.

4.3. Simulation Results of Injection Pressure Optimization. The study²⁸ indicates that the growth of the injection pressure results in a better urea atomization effect and a quicker evaporation and decomposition of urea. The effects of the optimized structure of scheme 1 on the urea injection pressure are studied. While the urea injection amount is unchanged, its injection time changes to change the injection pressure. The effects of the urea deposition rate, various uniformity coefficients, and the cumulative mass of liquid film are under study, while the injection pressure is 7, 9, 11, and 13 bar, respectively.

4.3.1. Results on the NH_3 Mass and the NH_3 Volume Fraction at the Front-End Cross Section of the SCR Catalyst. Effects of each injection pressure on the relations (total NH_3 mass at the front-end cross section of the SCR catalyst vs time, Figure 16) indicate that the growth of the injection pressure

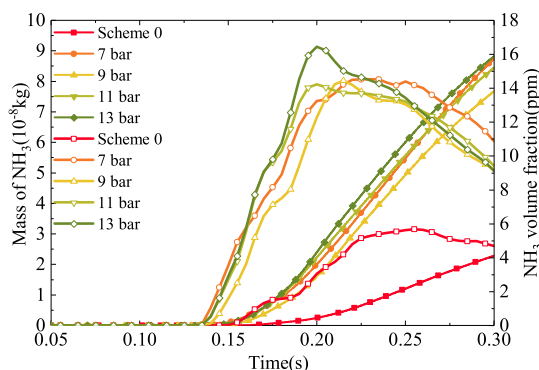


Figure 16. Mass of NH_3 and the NH_3 volume fraction at the front-end cross section of the SCR catalyst for each injection pressure.

can significantly improve the NH_3 mass and the NH_3 volume fraction at the front-end cross section of the SCR catalyst. While the injection pressure is 13 bar, at the front-end cross section of the SCR catalyst, the total NH_3 mass peaks at 8.82×10^{-8} kg. When the injection pressure is 7 bar, the mass of NH_3 is slightly lower than that of 13 bar, which is 8.75×10^{-8} kg, and after 0.23 s, the NH_3 volume fraction on the cross section is higher than other injection pressure conditions.

4.3.2. Results on the Uniformity. The uniformity coefficient of the SCR front-end cross section under each injection pressure (Figure 17) indicates that various uniformity

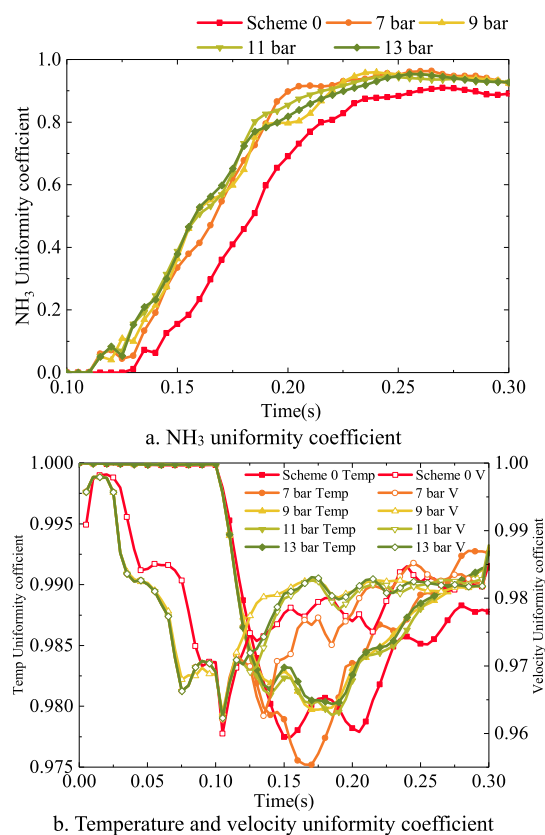


Figure 17. Uniformity coefficient curve for each injection pressure. (a) NH₃ uniformity coefficient. (b) Temperature and velocity uniformity coefficient.

coefficients also increase accordingly and NH₃ is more evenly distributed with the growth of the injection pressure. Instead, the change in injection pressure does not greatly affect the temperature and the velocity uniformity.

The average value of the uniformity coefficient of NH₃ between 0.25 and 0.3 s is 0.95, 0.94, 0.93, and 0.94, respectively.

4.3.3. Results on the Film Mass and Urea Deposition Rate.

The relation (liquid film mass vs. injection pressure, Figure 18) indicates that with the growth of the injection pressure, the cumulative mass of the liquid film decreases. The cumulative mass and maximum mass of the liquid film is minimum, while the injection pressure is 7 bar. For this model, too high

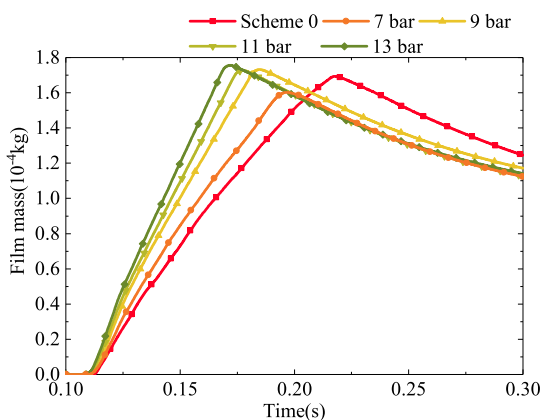


Figure 18. Liquid film mass at each injection pressure.

injection pressure will make the urea droplet collide with the wall prematurely and form the liquid film. Therefore, the injection pressure should be appropriately increased to meet the optimization requirements. Thus, the cumulative masses of the liquid film are 1.12, 1.17, 1.13, and 1.14 × 10⁻⁸ kg, respectively, and the urea deposition rates are 41.48, 43.33, 41.85, and 42.22%, respectively.

Figure 19 shows the film distribution of scheme 0 and scheme 1–7 bar. After the structure of the mixer is optimized,

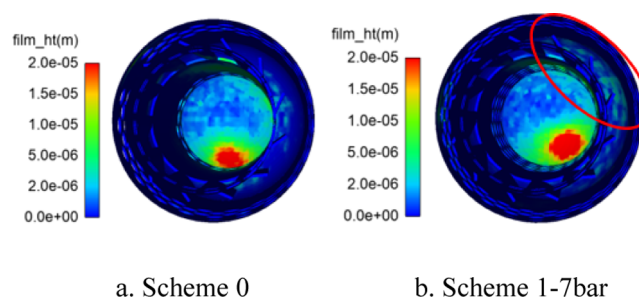


Figure 19. Film distribution of scheme 0 and scheme 1–7 bar. (a) Scheme 0. (b) scheme 1–7 bar.

the flow field in this region is also changed. The urea droplets may come into contact with the high-temperature wall (in Figure 18b, it is circled in a red line) which cannot be contacted by the previous structure, so it can decompose more NH₃ and reduce the mass of the liquid film.

Thus, selecting the mixer structure of scheme 1 and changing the injection pressure to 7 bar is the final optimized solution. Compared with the original scheme, the final optimization results are that the mass of the NH₃ and the NH₃ uniformity at the front-end cross section of the SCR catalyst increase by 2.83 times and 5.65%, and the urea deposition rate and the cumulative mass of the liquid film fall by 4.82 and 10.4%, respectively.

5. CONCLUSIONS

- (1) A corresponding CFD model was established based on the integrated after-treatment device of a certain engine, and the model is verified by experimental data. The results show that the error between the simulation value and the experimental value of pressure drop and wall temperature is low, and the distribution of the liquid film is basically consistent with the experiment, which shows that the model can well predict the urea crystallization.
- (2) The performance of four different mixers was evaluated by taking the uniformity coefficient of the front-end section of the SCR catalyst, the mass and volume fraction of NH₃, and liquid film accumulation mass of the mixer as indexes. The results show that the performance of scheme 1 is the best.
- (3) The injection pressure is studied based on the mixer structure of scheme 1, and the results show that for this model, too high injection pressure will make the urea droplet collide with the wall prematurely and form the liquid film. The mass and volume fraction of NH₃ and the NH₃ uniformity coefficient peak, but the urea deposition rate and the cumulative mass of the liquid film are minimum while the injection pressure is changed to 7 bar.

This study can provide a certain guidance on optimization design of structural parameters of this type of integrated after-treatment device.

AUTHOR INFORMATION

Corresponding Author

Xingyu Liu – Hubei Key Laboratory of Advanced Technology for Automotive Components, Wuhan University of Technology, Wuhan 430070, China; Hubei Collaborative Innovation Center for Automotive Components Technology, Wuhan University of Technology, Wuhan 430070, China; orcid.org/0000-0003-0677-7024; Email: liuxingyu@whut.edu.cn

Authors

Menghua Wang – State Key Laboratory of Power System of Tractor, Luoyang 471039, China; School of Energy and Power Engineering, Xi'an Jiaotong University, Xi'an 710049, China

Jianjun Bao – State Key Laboratory of Power System of Tractor, Luoyang 471039, China

Zhidan Li – State Key Laboratory of Power System of Tractor, Luoyang 471039, China

Jie Hu – Hubei Key Laboratory of Advanced Technology for Automotive Components, Wuhan University of Technology, Wuhan 430070, China; Hubei Collaborative Innovation Center for Automotive Components Technology, Wuhan University of Technology, Wuhan 430070, China

Complete contact information is available at:

<https://pubs.acs.org/10.1021/acsoomega.0c05785>

Notes

The authors declare no competing financial interest.

ACKNOWLEDGMENTS

This study is funded by the National Key R & D Program Funded Project (2017YFC0211203), Open Project of National Key Laboratory of Tractor Power System (AKT2019004), Hubei Provincial Natural Science Foundation (2018CFB592), Open Fund of National Engineering Laboratory for Mobile Pollution Source Emission Control Technology (NELMS2017A08), New Energy Automobile Science, Key Technology Discipline Innovation Intelligence Base Fund (B17034), Innovation Team Development Program of Ministry of Education (IRT_17R83), and Fundamental Research Funds for the Central Universities (2020III038).

REFERENCES

- (1) López, J. M.; Jiménez, F.; Aparicio, F.; Flores, N. On-road emissions from urban buses with SCR+Urea and EGR+DPF systems using diesel and biodiesel. *Transport. Res. Transport Environ.* **2009**, *14*, 1–5.
- (2) Rohr, F.; Grißtede, I.; Bremm, S. Concept Study for NOx Aftertreatment Systems for Europe. *SAE Technical Paper*, 2009(1): 632–642.
- (3) Williams, A.; McCormick, R.; Luecke, J.; Brezny, R.; Geisselmann, A.; Voss, K.; Hallstrom, K.; Leustek, M.; Parsons, J.; Abi-Akar, H. Impact of Biodiesel Impurities on the Performance and Durability of DOC, DPF and SCR Technologies. *SAE Int. J. Fuels Lubr.* **2011**, *4*, 110–124.
- (4) Han, D.; Yang, B. Comparison and Analysis of Exhaust Emission Regulation between EU6 and Stage 6 in China. *Automob. Appl. Technol.* **2017**, *4*, 191–193.

- (5) Shahariar, G. M. H.; Lim, O. T. A Study on Urea-Water Solution Spray-Wall Impingement Process and Solid Deposit Formation in Urea-SCR de-NOx System. *Energies* **2018**, *12*, 125.

- (6) Su, C. Commercial Vehicle Post-processing system of Urea Crystallization Problem Research. *Automob. Appl. Technol.* **2016**, *10*, 223–226.

- (7) Tan, L.; He, L.; Kou, C.; Jiang, J.; Gong, J. Numerical Simulation on Spray Atomization of Diesel Engine Urea-SCR System. *Chin. J. Environ. Eng.* **2014**, *8*, 1554–1560.

- (8) Zhu, M.; Hu, Z.; Xia, S.; Ju, Y.; Lyu, J. Evaluation and Prediction About the Risk of Urea Deposits in the SCR System. *Trans. CSICE* **2020**, *38*, 90–95.

- (9) Roy, S.; Barman, J.; Khan, R. Development of Air less Urea Dozing Architecture for Better Optimum Spray Characteristics and to Avoid Urea Crystallization. *SAE Technical Paper*, 2017-28-1927, 2017.

- (10) Jain, A.; Barman, J.; Patchappalam, K.; Gedela, S. Study on the Factors Affecting the Formation of Urea Crystals and its Mitigation for SCR After-Treatment Systems. *SAE Technical Paper*, 2017-26-0132, 2017.

- (11) Grout, S.; Blaisot, J.-B.; Pajot, K.; Osbat, G. Experimental investigation on the injection of an urea-water solution in hot air stream for the SCR application: Evaporation and spray/wall interaction. *Fuel* **2013**, *106*, 166–177.

- (12) Tischer, S.; Börnhorst, M.; Amsler, J.; Schoch, G.; Deutschmann, O. Thermodynamics and reaction mechanism of urea decomposition. *Phys. Chem. Chem. Phys.* **2019**, *21*, 16785.

- (13) Chen, Y.; Huang, H.; Li, Z.; Wang, H.; Hao, B.; Chen, Y.; Huang, G.; Guo, X. Study of reducing deposits formation in the urea-SCR system: Mechanism of urea decomposition and assessment of influential parameters. *Chem. Eng. Res. Des.* **2020**, *164*, 311–323.

- (14) Huang, H.; Chen, Y.; Li, Z.; Wang, H.; Hao, B.; Chen, Y.; Lei, H.; Guo, X. Analysis of deposit formation mechanism and structure optimization in urea-SCR system of diesel engine. *Fuel* **2020**, *265*, 116941.

- (15) Shahariar, G. M. H.; Jo, H.; Lim, O. Analysis of the spray wall impingement of urea-water solution for automotive SCR De-NOx systems. *Energy Procedia* **2019**, *158*, 1936–1941.

- (16) Luo, Z.; Sukheswalla, P.; Drennan, S. A.; Wang, M. 3D Numerical Simulations of Selective Catalytic Reduction of NOx With Detailed Surface Chemistry. *Asme Internal Combustion Engine Division Fall Technical Conference*, 2017.

- (17) Zheng, G. CFD Modeling of Urea Spray and Deposits for SCR Systems. *SAE Technical Paper*, 2016.

- (18) Praveena, V.; Martin, L. J. Design Optimization of Urea Injectors and Mixers in a Compact SCR System. *SAE Technical Paper*, 2018.

- (19) Koebel, M.; Elsener, M. Selective catalytic reduction of NO over commercial DeNOx-catalysts: experimental determination of kinetic and thermodynamic parameters. *Chem. Eng. Sci.* **1998**, *53*, 657–669.

- (20) Kim, J. Y.; Ryu, S. H.; Ha, J. S. Numerical prediction on the characteristics of spray induced mixing and thermal decomposition of urea solution in SCR system. *Asme Internal Combustion Engine Division Fall Technical Conference*, 2004.

- (21) Birkhold, F.; Meingast, U.; Wassermann, P.; Deutschmann, O. Modeling and simulation of the injection of urea-water-solution for automotive SCR DeNOx-systems. *Appl. Catal., B* **2007**, *70*, 119–127.

- (22) Wen, S.; Jia, H.; Li, X. Influence of Structure of Urea-SCR Injection System on Spray and Mixing Characteristics at Low Exhaust Temperature. *Mach. Des. Manufact.* **2018**, *A2*, 101–104.

- (23) Chatterjee, D.; Kočí, P.; Schmeißer, V.; Marek, M.; Weibel, M.; Krutzsch, B. Modelling of a combined NOx storage and NH3-SCR catalytic system for Diesel exhaust gas aftertreatment. *Catal. Today* **2010**, *151*, 395–409.

- (24) O'Rourke, P. J.; Amsden, A. A. The TAB Method for Numerical Calculation of Spray Droplet Breakup. *SAE Technical Paper*, 872089, 1987.

- (25) Maciejewski, D.; Sukheswalla, P.; Wang, C.; Drennan, S. A.; Chai, X. Accelerating Accurate Urea/SCR Film Temperature

Simulations to Time-Scales Needed for Urea Deposit Predictions. *SAE Technical Paper* 2019-01-0982, 2019.

(26) Wruck, N.; Renz, U. Transient phase-change of droplets impacting on a hot wall. *Transient Phenomena in Multiphase and Multicomponent Systems: Research Report*; Wiley-VCH Verlag GmbH & Co. KGaA, 2007.

(27) Weltens, H.; Bressler, H.; Terres, F.; Neumaier, H.; Rammoser, D. Optimisation of Catalytic Converter Gas Flow Distribution by CFD Prediction. *SAE Technical Paper* 930780, 1993.

(28) Wang, J.; Wang, Q.; Xu, H.; Zhao, W.; Wu, L.; Li, S. Influential Factors on NO_x Conversion Efficiency of Vehicle SCR System. *Trans. CSICE* **2015**, *33*, 453–460.